



Published in final edited form as:

Cell Rep Phys Sci. 2023 September 20; 4(9): . doi:10.1016/j.xcrp.2023.101513.

Rapid and accurate detection of herpes simplex virus type 2 using a low-cost electrochemical biosensor

Lucas F. de Lima^{1,2,3,4,7}, André L. Ferreira^{1,2,3,4,7}, Sita Awasthi⁵, Marcelo D.T. Torres^{1,2,3}, Harvey M. Friedman⁵, Gary H. Cohen⁶, William R. de Araujo^{4,*}, Cesar de la Fuente-Nunez^{1,2,3,8,*}

¹Machine Biology Group, Departments of Psychiatry and Microbiology, Institute for Biomedical Informatics, Institute for Translational Medicine and Therapeutics, Perelman School of Medicine, University of Pennsylvania, Philadelphia, PA, USA

²Departments of Bioengineering and Chemical and Biomolecular Engineering, School of Engineering and Applied Science, University of Pennsylvania, Philadelphia, PA, USA

³Penn Institute for Computational Science, University of Pennsylvania, Philadelphia, PA, USA

⁴Portable Chemical Sensors Lab, Department of Analytical Chemistry, Institute of Chemistry, State University of Campinas – UNICAMP, Campinas, São Paulo, Brazil

⁵Infectious Disease Division, Department of Medicine, Perelman School of Medicine, University of Pennsylvania, Philadelphia, PA, USA

⁶Department of Basic and Translational Sciences, School of Dental Medicine, University of Pennsylvania, Philadelphia, PA, USA

⁷These authors contributed equally

⁸Lead contact

SUMMARY

Herpes simplex virus type 2 (HSV-2) infection, which is almost exclusively sexually transmitted, causes genital herpes. Although this lifelong and incurable infection is extremely widespread,

*Correspondence: wra@unicamp.br (W.R.d.A.), cfuente@upenn.edu (C.d.l.F.-N.), <https://doi.org/10.1016/j.xcrp.2023.101513>.

AUTHOR CONTRIBUTIONS

Conceptualization, M.D.T.T., H.M.F., G.H.C., and C.F.N.; methodology, L.F.d.L., A.L.F., S.A., and W.R.d.A.; investigation, L.F.d.L., A.L.F., and S.A.; writing – original draft, L.F.d.L., A.L.F., W.R.d.A., and C.F.N.; writing – review & editing, L.F.d.L., A.L.F., S.A., M.D.T.T., H.M.F., G.H.C., W.R.d.A., and C.F.N.; resources, G.H.C. and C.F.N.; supervision, W.R.d.A. and C.F.N. The manuscript was written through contributions from all authors. All authors have given approval to the final version of the manuscript.

SUPPLEMENTAL INFORMATION

Supplemental information can be found online at <https://doi.org/10.1016/j.xcrp.2023.101513>.

DECLARATION OF INTERESTS

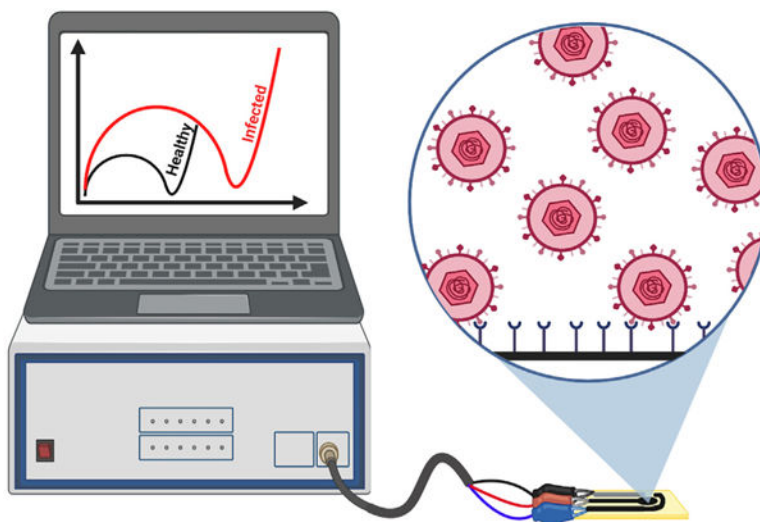
A non-provisional patent application has been filed on the de la Fuente Lab's related work (ID number 23–10377). C.F.N. provides consulting services to Invaio Sciences and is a member of the Scientific Advisory Boards of Nowture S.L. and Phare Bio. The de la Fuente Lab has received research funding or in-kind donations from United Therapeutics, Strata Manufacturing PJSC, and Procter & Gamble, none of which were used in support of this work. C.F.N. is on the Advisory Board of *Cell Reports Physical Science*.

INCLUSION AND DIVERSITY

One or more of the authors of this paper self-identifies as an underrepresented ethnic minority in their field of research or within their geographical location. One or more of the authors of this paper self-identifies as a gender minority in their field of research. One or more of the authors of this paper received support from a program designed to increase minority representation in their field of research. We support inclusive, diverse, and equitable conduct of research.

currently there is no readily available diagnostic device that accurately detects HSV-2 antigens to a satisfactory degree. Here, we report an ultrasensitive electrochemical device that detects HSV-2 antigens within 9 min and costs just \$1 (USD) to manufacture. The electrochemical biosensor is biofunctionalized with the human cellular receptor nectin-1 and detects the glycoprotein gD2, which is present within the HSV-2 viral envelope. The performance of the device is tested in a guinea pig model that mimics human biofluids, yielding 88.9% sensitivity, 100.0% specificity, and 95.0% accuracy under these conditions, with a limit of detection of 0.019 fg mL^{-1} for gD2 protein and $0.057 \text{ PFU mL}^{-1}$ for titered viral samples. Importantly, no cross-reactions with other viruses were detected, indicating the adequate robustness and selectivity of the sensor. Our low-cost technology could facilitate more frequent testing for HSV-2.

Graphical Abstract



Here, de Lima and Ferreira et al. describe an electrochemical biosensor capable of detecting herpes simplex virus type 2 antigens within 9 min. This low-cost diagnostic test presents excellent analytical performance on animal samples.

INTRODUCTION

Both types of herpes simplex virus (HSV), HSV-1 and HSV-2, are prevalent in humans and cause neonatal infections.¹ Furthermore, these viruses can establish lifelong latency in the sensory neuronal ganglia. Subsequent reactivation of latent virus may cause significant health problems and result in viral transmission to healthy individuals. HSV-1, also known as oral herpes, infects the lips, mouth, eyes, and brain; while HSV-2, also known as genital herpes, is associated mainly with genital infections.²

The World Health Organization (WHO) recently estimated the global prevalence of HSV-1 in individuals aged 0–49 years to be 66.6%, or more than 3.7 billion people who have been infected by HSV-1.¹ Additionally, the WHO estimates the global prevalence of HSV-2, which is transmitted almost exclusively through sexual contact, to include 13.2% of the world's population, or 491.6 million people aged 15–49 years. The attachment of the virus

to the cell surface initially involves two glycoproteins on the HSV envelope, glycoprotein C (gC), and to a lesser extent, glycoprotein B (gB).³⁻⁵ Glycoprotein D (gD), found within the viral envelope, then binds to host cell receptors, initiating a sequence of events that allows HSV to fuse with the host's cell plasma membrane.⁶ Studies of the binding of gD to cell surface receptors have led to an understanding of the interaction between human cell receptors and HSV.^{5,7-9}

Despite the prevalence of HSV-2 infections, there are currently no rapid tests available to detect this infectious agent. Historically, viral culturing has been the main test used for HSV detection in the clinic.¹⁰ However, recently, molecular methods such as polymerase chain reaction (PCR) have been widely used in clinical practice due to their increased sensitivity and selectivity compared to viral culture.^{10,11} Currently, there are very few FDA-cleared molecular tests available for HSV detection. Examples include PCR-based MultiCode-RTx kit, ProbeTec HSV Qx test, and IsoAmp HSV assay with sensitivity and selectivity ranging from 92.4% to 98.4% and 83.7% to 97.0%, respectively. Other commercial serological methods such as immunoblot, ELISA, western blotting, and chemiluminescence immunoassay have also been used to detect HSV.¹²⁻¹⁴ However, immunoassays rely on the availability of HSV antibodies, and thus, the sensitivity of these tests is influenced by the amount of time since the infection. Indeed, immunoassays display the highest sensitivity when performed at least 21 days after the initial infection and may improve if performed more than 40 days after the primary infection,¹¹ thus clearly hindering early HSV diagnosis. In addition, these diagnostic methods are time-consuming, costly, and laborious, requiring highly trained staff and sophisticated laboratory infrastructure.

Rapid and accessible diagnostic technologies could improve the management of HSV infections, particularly in low-resource settings and in labor and delivery wards.^{2,15-17} In fact, several portable devices have been reported as alternative methods for the diagnosis of HSV, and electrochemical detection methods are attractive for developing such devices. Electrochemical detection has adequate sensitivity and selectivity and can be associated with accessible and portable instrumentation.¹⁸ Generally, these portable diagnostic devices are DNA-based biosensors aiming to detect viral genetic material.¹⁸ Detecting viral DNA or RNA present in biofluids can lead to base-pairing mismatches and hybridization problems that compromise the selectivity of the tests. Moreover, these methods commonly require preconcentration or amplification protocols to achieve the desired sensitivity, decreasing the ability to conduct rapid, frequent, and inexpensive tests.¹⁸

Rapid and accessible diagnostic technologies constitute promising approaches to help manage HSV-2 infections. Here, we describe an impedimetric biosensor for the rapid, ultrasensitive detection of HSV-2 (Figure 1A). Instead of traditional genosensors and serological tests, we report the use of nectin-1 as a cellular receptor¹⁹ for the development of an accurate electrochemical diagnostic for HSV-2. Our simple technology uses carbon screen-printed electrodes functionalized with the conductive polymer polyethyleneimine (PEI), the bioreceptor nectin-1, and a chitosan semipermeable membrane (Figure 1B). In order to develop a sensitive and robust rapid test, in our study, we carefully evaluated each functionalization step, investigating the optimal strategy to biofunctionalize the working electrode. Under optimal conditions, our device detected the virus within 9 min (sample

incubation + analysis), displayed a limit of detection (LOD) of 0.057 plaque-forming units (PFU) mL⁻¹, and presented 88.9% sensitivity, 100% specificity, and 95% accuracy when tested on 20 pre-clinical samples from the guinea pig vaginal canal (11 negative samples and 9 positive samples).

RESULTS AND DISCUSSION

Development and performance of the HSV-2 biosensor

In our study, we used electrochemical impedance spectroscopy (EIS) for the transduction of the biosensor response, i.e., the selective binding between the nectin-1 bioreceptor immobilized on the electrode surface and the gD2 glycoproteins from HSV-2. The binding between nectin-1 and gD2 changes the interfacial electron transfer kinetics between ferricyanide/ferrocyanide (i.e., the redox probe used) and the electrode. The altered kinetics, in turn, can be detected by monitoring the increase in resistance to charge transfer (R_{CT}), indicating a positive diagnostic result for HSV-2 infection (Figure 1A), similar to the previous work.²⁰ We carefully studied each functionalization step to generate a reliable, ultrasensitive, and robust biosensor that presents original functional materials for HSV-2 diagnosis (Figure 1B). The R_{CT} values were extracted by application of the Randles equivalent electrical circuit.²¹

All data from the optimization studies and analytical curves were plotted using the normalized R_{CT} response, as defined by the following equation:

$$\text{Normalized } R_{CT} = \frac{Z - Z_0}{Z_0},$$

(Equation 1)

where Z is the R_{CT} value obtained after incubating the electrode surface with gD2 or HSV-2 samples, and Z_0 is the R_{CT} value of the analytical blank solution (i.e., phosphate buffer saline [PBS] or Dulbecco's Modified Eagle Medium [DMEM] with 5% fetal bovine serum [FBS]). The normalization process of R_{CT} corrects variations in the sensor response, which may be caused by analyst operation and temperature fluctuations when testing. Thus, normalization facilitates the eventual use of the sensor at decentralized testing sites.²⁰

Initially, to generate a robust and sensitive biosensor, two strategies were evaluated to modify the working electrode (WE) and enable the anchoring of the nectin-1 bioreceptor. In the first approach, the WE surface was coated with glutaraldehyde (GA), a dialdehyde widely used to anchor biomolecules through their N-terminal groups²²; for the second approach, the WE was modified with PEI, a conductive polymer containing amino functional groups enabling the attachment of biomolecules through their carboxylic acid and ester groups.^{23,24} Using GA as a modifier did not provide significant discrimination of the analytical signal (R_{CT}) at the concentrations of gD2 tested (10^{-12} – 10^{-9} g mL⁻¹, Figure 2A). This result can be explained by the partial obstruction, or steric effect on the active sites, present in the domain of the receptor when this immobilization strategy was used, which may have hindered the effective interaction with the viral particle. This hypothesis was confirmed by our observation that the PEI modification allowed detection of the binding

interactions between nectin-1 and gD2, yielding the high sensitivity seen in the analytical curve (Figure 2A). The binding of the C terminus of nectin-1 to the PEI-modified surface left the –NH groups of the former free for gD2 to interact with.⁶

We next optimized the main fabrication, modification, and functionalization steps of the biosensor using PEI. First, the WE was modified with 4.0 μL of 1.0 mg mL^{-1} PEI solution, by drop-casting, and incubated for 60 min at 37°C. This procedure generates –NH functional groups on the carbon electrode surface.^{25–27} Then, 4.6 mL of 0.13 mg mL^{-1} of the nectin-1 receptor, containing a mixture of 25.0 mmol L^{-1} N-(3-dimethylaminopropyl)-N-ethylcarbodiimide hydrochloride (EDC) + 50.0 mmol L^{-1} N-hydroxysuccinimide (NHS), was deposited on the surface of the PEI-modified WE, and the biosensor was incubated for 30 min at 37°C. The carboxyl groups on nectin-1, when exposed to EDC-NHS, are activated to form a stable ester, which undergoes a nucleophilic addition with the amino groups on the PEI-modified WE, such that a stable amide bond is formed between the PEI-modified carbon electrode and nectin-1.²³ Subsequently, the remaining unmodified sites of the electrode surface were blocked with 4.0 μL of a 1.0% (m/v) bovine serum albumin (BSA) solution. In the last step, 4.0 μL of 0.5% (m/v) chitosan was dropped on the surface of the nectin-1-modified WE. Chitosan is a polyelectrolyte semipermeable membrane that presents several advantages as a coating material in the development of biosensors, such as permeability, biocompatibility, hydrophilicity, and the presence of –NH₂ and –OH functional groups that enable immobilization of biomolecules through covalent binding or electrostatic interactions. In addition, chitosan forms hydrogel films that provide differential mass transport with preconcentration of some ions and organic molecules, as well as protective features to the transducer/receptor surface, conferring robustness to the biosensors.^{28–31}

After selecting PEI as the optimal immobilization strategy for nectin-1, we evaluated the use of two types of permeable membranes, namely Nafion and chitosan. Analytical curves ranging from 1×10^{-12} to 1×10^{-10} g mL^{-1} of gD2 in 0.1 mol L^{-1} of PBS (pH = 7.4) were constructed. Experiments were performed in triplicate to compare three strategies: (1) without a permeable membrane, (2) with 0.5% Nafion, and (3) with 0.5% chitosan (Figure 2B). According to these results, the electrochemical biosensor modified with chitosan 0.5% (m/v) presented a sensitivity of 0.222, which is 1.6-fold higher than the biosensor without any semipermeable membrane (sensitivity of 0.138) and 2.74-fold higher than the biosensor with Nafion (sensitivity of 0.081). The increase in sensitivity is associated with the preconcentration features of the glycoprotein gD2 during the incubation period, which is trapped close to the bioreceptor, enabling a larger number of binding events and enhancing the detectability of our method (Figure 2B). In addition, the positive charges displayed by chitosan in the acidic medium can preconcentrate $[\text{Fe}(\text{CN})_6]^{3-/4-}$, i.e., the anionic redox probe, into the polymeric layer, enhancing the electrochemical response.^{32,33} Given these results, we studied the proportion of chitosan on the modified biosensor since it directly impacts membrane thickness. Our experiments revealed that 0.5% (m/v) of chitosan provided the highest impedimetric responses and analytical sensitivity since higher concentrations provided lower detectability (Figure 2C). Thus, 0.5% (m/v) of chitosan was selected for further studies.

Subsequently, we evaluated the optimal incubation time of either gD2 or viral samples with the surface of the biosensor to obtain the optimal compromise between analytical frequency and sensitivity for HSV-2 detection. The optimization was based on the analytical sensitivity (slope) parameter obtained by analytical curves, determined in triplicate, at concentrations of gD2 ranging from 10^{-12} to 10^{-10} g mL⁻¹ (Figure 2D). By balancing detection ability with the sensitivity values of the dose-response curves while maintaining a short testing time, we selected 5 min as the optimal incubation time. These results demonstrate the rapid binding kinetics between gD2 and the immobilized nectin-1 on the electrode surface, underscoring the efficiency of our functionalized biosensor architecture.

Electrochemical characterization of the biosensor

For each functionalization step (Figure 3A), the electrochemical behavior was characterized by cyclic voltammetry (CV) and EIS (Figures 3B and 3C, respectively). CV (Figure 3B) and Nyquist (Figure 3C) plots show that the bare carbon electrode (black line) presented poorly defined redox processes with peak currents (*ip*) of 133.1 ± 2.5 μ A and R_{CT} of 549.4 ± 24.6 Ω . The electrochemical performance of the sensor was enhanced by modifying the carbon electrode surface with PEI (red line), as well-defined and intense (251.71 ± 3.17 μ A) current peaks were observed for the redox probe with an R_{CT} value of 11.1 ± 1.2 Ω . These results were expected, given the high charge transfer generated by the π -electrons of the conductive PEI membrane.³⁴ Next, nectin-1 was anchored to the electrode surface using the EDC-NHS approach (blue line). The receptor was first immobilized through an amide bond between the amine group from the PEI and the carboxyl groups from nectin-1.³⁵ This step led to a small increase in the R_{CT} value, to 17.6 ± 2.1 Ω , and a slight decrease of the *ip*, to 247.15 ± 2.56 μ A (blue line). Any nonspecific sites of the electrode were blocked by using 1.0% (m/v) BSA solution, resulting in an R_{CT} of 26.3 ± 1.2 Ω and *ip* of 231.2 ± 3.9 μ A (magenta line) due to the introduction of a nonconductive layer on the surface of the electrode. Finally, the electrode surface was modified with a 0.5% (m/v) chitosan permeable membrane to enhance the robustness and sensitivity of the biosensor. This step increased the R_{CT} to 47.5 ± 4.0 Ω and decreased the *ip* to 222.0 ± 3.3 μ A (green line).

Analytical performance of the biosensor

EIS was used to quantify free gD2 and HSV-2 virus in 0.1 mol L⁻¹ PBS (pH = 7.4). Dose-response curves were built with our previously optimized experimental conditions (i.e., 1 mg mL⁻¹ PEI, 0.5% chitosan, and 5 min of incubation time), and the analytical results were normalized according to Equation 1. Figure 4A illustrates Nyquist plots for increased concentrations of gD2 ranging from 0.1 fg mL⁻¹ to 10.0 ng mL⁻¹ in 0.1 mol L⁻¹ PBS (pH = 7.4). A linear correlation was observed over the entire range of concentrations evaluated (0.1 fg mL⁻¹ to 10.0 ng mL⁻¹ gD2), when plotted as a logarithm function (Figure 4B), with a determination coefficient R^2 of 0.997. The LOD and limit of quantification (LOQ) were calculated as 0.019 fg mL⁻¹ and 0.089 fg mL⁻¹ gD2, respectively. We also built an analytical curve for a titrated HSV-2 sample at concentrations, in a DMEM medium, ranging from 1×10^0 to 1×10^7 PFU mL⁻¹ (Figure 4C). A linear correlation was observed in the concentration range from 1×10^0 PFU mL⁻¹ to 1×10^5 PFU mL⁻¹ with an $R^2 = 0.999$ (Figure 4D). LOD and LOQ were calculated as 0.057 PFU mL⁻¹ and 0.210 PFU mL⁻¹ HSV-2, respectively. Three different biosensors were used per experiment, and

concentrations were depicted as the logarithmic function of the dose used for gD2 and HSV-2. The four-parameter logistic curve (Figure S1),³⁶ a method that assesses binding interactions and kinetics,^{22,37} was used to determine the LOD and LOQ values.

Collectively, these experiments highlight the excellent sensitivity displayed by our biosensor, which we anticipate can provide an early diagnosis of HSV-2 infection in human clinical samples. Another advantage that our biosensor has for diagnostic purposes is its short testing time, i.e., 9 min, consisting of a 5-min incubation of the sample on the electrode surface and an additional 4 min for the EIS measurements of both the analytical blank and the sample of interest.

In comparison to other methods reported in the literature (Table 1), our method is the first report, to the best of our knowledge, of the use of nectin-1 as a bioreceptor to detect the viral glycoprotein gD2 instead of genosensor technology using genetic material for the recognition of HSV. In addition, our sensor presents the fastest testing time, with a very low LOD and a large interval concentration range to detect HSV-2. Furthermore, our device can be produced inexpensively. Considering the cost of nectin-1 (\$800/mg), the final cost to assemble each HSV biosensor was exactly \$1.00 (USD): \$0.12 for electrode fabrication + \$0.40 for all the chemicals used in the functionalization step (PEI + EDC + NHS + BSA + chitosan) + \$0.48 for nectin-1. Because our biosensor is low-cost, its production is potentially highly scalable. Potential disadvantages of our method for point-of-care applications are primarily related to the use of a potentiostat that requires some expertise to use, the need for a redox probe solution to obtain the electrochemical response used for diagnostic purposes, and the specific software needed to interpret the results. Altogether, these disadvantages may limit the use of our current setup in testing sites where a trained person ideally would perform the test using multiplexed equipment with implemented routine analysis for frequent testing.

We also studied the effect on the biosensor's electrochemical response of adjusting the pH of the medium to a pH that is close to physiological conditions (Figure S2). DMEM medium was used to dilute the titered virus samples, and each pH value was adjusted to the range of 7.1–7.7 and tested using the optimized protocol previously described. When the pH of DMEM was 7.1, the biosensor exhibited a high detectability and a sensitivity of 0.212 ± 0.008 . At pH 7.4, sensitivity increased to 0.263 ± 0.003 . Finally, when the pH of DMEM was 7.7, the analytical sensitivity of the biosensor decreased (0.207 ± 0.008). These data can be explained by conformational changes of the biomolecules induced by differences in pH that, in turn, affect the binding of gD2 to the nectin-1 receptor. These results indicate the importance of adjusting the pH of biofluids for diagnostic purposes, for example, by using a buffered medium, since genital samples are usually acidic.^{6,51} Our results are consistent with previous studies evaluating the effect of pH changes on the interaction between gD2 and the nectin-1 receptor, which found that the alkalinity of the medium changed the proximity between the viral bilayer and the host cell membrane, likely affecting the interaction between nectin-1 and gD2. These changes influence the ability of the virus to fuse with and infect the cells.^{6,51}

Reproducibility and stability assays

To verify the reproducibility of the proposed method, i.e., to assess whether different batches of biosensors performed similarly, we evaluated six biosensors from different fabrication rounds using the same optimized protocol. Briefly, the R_{CT} measures were recorded by EIS using $5 \text{ mmol L}^{-1} [\text{Fe}(\text{CN})_6]^{3-/4-}$ after incubating the biosensor with $1 \times 10^{-9} \text{ g mL}^{-1}$ of gD2 prepared in 0.1 mol L^{-1} of PBS (pH = 7.4) (Figure S3). A relative standard deviation (RSD) of 5.12% was obtained, indicating excellent reproducibility of our manufacturing and biofunctionalization protocol. The experiments were carried out by incubating $10 \mu\text{L}$ of sample diluted in 0.1 mol L^{-1} PBS (pH = 7.4) for 5 min before recording each measurement.

The stability of the electrochemical biosensor, stored in sealed Petri plates at various temperatures (-20°C , 4°C , and 25°C), was evaluated over 7 days. Analytical curves were built at concentrations ranging from $1 \times 10^{-12} \text{ g mL}^{-1}$ to $1 \times 10^{-9} \text{ g mL}^{-1}$ gD2 in 0.1 mol L^{-1} PBS, pH 7.4 (Figure S4). The biosensors did not exhibit stability when stored at room temperature overnight. When stored at -20°C , on the other hand, the biosensors were stable for up to 72 h, but after 120 h, the sensitivity decreased to 48% of the initial value. The freezing of the biosensor for prolonged periods may modify the structuring of the functionalized surface, changing its ability to recognize the virus, i.e., the sensitivity. In this regard, electrodes stored at 4°C , the intermediary condition tested, were stable for 120h (5 days). The mean sensitivity of the device decreased after 7 days, displaying only 40% of the initial performance of the device. These results demonstrate that our biosensor has better stability if it is refrigerated at 4°C ; thus, refrigeration would be a convenient way to store our devices for decentralized applications.

Detection of HSV-2 in a pre-clinical animal model

Next, we assessed the ability of our biosensor to detect HSV-2 in 20 pre-clinical samples. We tested blindly, in triplicate ($n = 3$), 9 HSV-2-positive and 11 HSV-2-negative biofluid samples collected from the vagina of guinea pigs at the University of Pennsylvania (Figure 5). All samples were heat-inactivated (56°C for 1 h) prior to the electrochemical analysis. All samples were obtained from guinea pigs that had been infected 2 days earlier with HSV-2 or that were uninfected. The biosensor performance is dependent on the cutoff used to discriminate positive and negative samples. A low cutoff can enable the detection of low viral loads but may lead to false positive results. On the other hand, high cutoff values avoid false positive results but limit the detectability of the method, i.e., lead to false negative results.⁵² For diagnostic purposes, we set the cutoff value of our biosensor as $[(Z - Z_0)/Z_0] > 0.22$ to identify a positive HSV-2 result and $[(Z - Z_0)/Z_0] < 0.22$ for negative samples. The cutoff value was based on the analytical signal obtained for the lowest quantity of titrated virus analyzed (Figure 4D). Our biosensor achieved 88.9% sensitivity, 100% specificity, and 95% accuracy for the set of 20 samples evaluated, i.e., our biosensor correctly diagnosed 19/20 samples tested. However, increasing the number of clinical samples could impact the sensitivity, specificity, and accuracy of the proposed method. We note a response variation between the proposed method and the titrated method for sample analyses (Figure 5). This is likely due to the heat inactivation process prior to performing the electrochemical measurements, since heat inactivation induces viral lysis, generating different amounts of free gD2 or cell fragments containing gD2 that can interact

with the nectin-1 present on the surface of the WE. In addition, the heating step needs to be carefully performed to avoid denaturation of the glycoproteins, i.e., structural alterations on viral proteins (gD2).⁵³ Thus, these points prevent an exact correlation between the titrated method and our approach. However, based on the data obtained, we consider that the high diagnostic accuracy (95%) observed for the 20 samples tested suggests that our selective biosensor approach is excellent at detecting HSV-2 viral particles in complex samples and thus constitutes a promising alternative to standard methods.

Cross-reactivity experiments

We performed cross-reactivity experiments to rule out any potential off-target effects of our nectin-1-modified electrode with viruses other than HSV. Selectivity was studied for five viruses: H1N1 (A/California/2009), influenza B (B/Colorado), influenza A H3N2, MHV-mouse hepatitis virus, and SARS-CoV-2. All experiments were performed using the same optimized conditions as those used for HSV-2 detection. No significant cross-reactivity was detected with any of the viruses tested, as revealed by a relative R_{CT} percentage of up to 12%, which is lower than the cutoff value of 22% established for a positive diagnosis of HSV-2 infection in biofluid samples (Figure S5). These results, associated with the selectivity observed in the analysis of pre-clinical samples (guinea pig vaginal biofluids) in which no false positives were detected, highlight the robustness and selectivity of our biosensor. However, the glycoprotein D proteins from HSV-1 and HSV-2 have a high degree of identity, and both viruses can enter the cell through gD binding to the nectin-1 receptor, which could result in the detection of HSV-1 if that virus were present in genital biofluid or the clinical sample tested. Our device can be advantageous to diagnose both HSV-1 and HSV-2 infections. A relevant scenario for the use of such a testing device could be in pregnant women in labor before childbirth if the presence of either HSV-1 or HSV-2 is suspected. Such a diagnosis can help prevent the newborn from acquiring neonatal herpes from an infected mother.

In summary, we have developed an electrochemical biosensor for the ultrasensitive detection of HSV-2 antigen, using nectin-1 as the receptor. In fact, this is the first electrochemical approach that uses nectin-1 as a recognition element instead of the well-established DNA-based strategy. Our approach is substantially less complex than DNA-based methods as the analytical steps do not require amplification or hybridization. With this device, the detection of viral antigen requires only minimal amounts of sample (10 μ L). The biosensor can be prepared in less than 3 h, and when stored at 4°C, it remains stable for at least 5 days. Furthermore, the process of detection takes only 9 min. The sample is incubated on the electrode surface for the first 5 min, and the analytical blank and the sample are measured by EIS within 4 min. Our simple manufacturing and biofunctionalization method provides a biosensor with reproducible (RSD = 5.12%) and excellent analytical features for detecting HSV-2 (LODs of 0.019 fg mL^{-1} for free gD2 in PBS medium and 0.057 PFU mL^{-1} for titered virus in DMEM). Collectively, our method provides an excellent alternative for HSV diagnosis since it does not require the amplification and hybridization steps that are commonly used in DNA-based methods. Its low cost (\$1.00 USD test) and speed of detection can allow frequent tests for screening of the population, mainly in resource-limited settings and labor and delivery wards. In our analysis of 20 guinea pig vaginal biofluid

samples, the biosensor accurately detected 8/9 HSV-2 positive samples and 11/11 negative samples, achieving 88.9% sensitivity, 100% specificity, and 95% accuracy. In conclusion, we present an inexpensive, rapid, and accurate technology for diagnosing HSV-2 antigen in relevant biological samples.

EXPERIMENTAL PROCEDURES

Resource availability

Lead contact—C.F.N. is the lead contact; e-mail address: cfuente@upenn.edu.

Materials availability—Sensors generated in this study will be made available upon reasonable request.

Data and code availability—All the data generated in this study will be made available upon reasonable request.

Chemicals and apparatus

Analytical-grade reagents were used for the experiments. Deionized water (resistivity 18 M Ω cm at 25°C) was obtained from a Milli-Q Advantage-0.10 purification system (Millipore). Human herpes virus entry mediator (HveC), also called human nectin-1 (residues 31–346), and gD2 strain 333 (residues 1 to 285, gD(285t)) proteins were recombinantly produced by baculoviruses. Their purification from infected insect cells was described previously.^{54,55} EDC, NHS with a degree of purity 98%, BSA, chitosan (molecular weight = ~50,000 Da), PBS solution, pH = 7.4, and glutaraldehyde (25%, v/v) were purchased from Sigma-Aldrich. PEI was obtained from Polysciences. Carbon and Ag/AgCl conductive inks were obtained from Creative Materials. A six-channel MULTI AUTOLAB M101 potentiostat operated by the NOVA 2.1 software was used for the electrochemical measurements.

Electrochemical measurements

All electrochemical measurements were carried out using a mixture of 5.0 mmol L⁻¹ [Fe(CN)₆]³⁻ and [Fe(CN)₆]⁴⁻, as a redox probe, in 0.1 mol L⁻¹ KCl solution. All functionalization steps of the biosensor were characterized by EIS, which was also used to quantify the HSV-2 and gD2 concentrations. The frequencies used ranged from 1 × 10⁵ Hz to 0.1 Hz, and the open circuit potential was applied with an amplitude of 10 mV (vs. Ag/AgCl). For CV experiments, the potential ranged from -0.3 to 0.7 V (vs. Ag/AgCl) using a scan rate of 50 mV s⁻¹.

Fabrication of electrochemical devices

The electrochemical sensors (three-electrode configuration) were manufactured by a screen-printing technique on phenolic paper circuit board material, as a low-cost and convenient platform.²⁰ Electrically conductive carbon and Ag/AgCl inks (Creative Materials, USA) were employed to construct the working (WE)/auxiliary (AE) and reference (RE) electrodes, respectively. After a curing step of 30 min at 100°C, the material was cut into 2.5 × 2.0 cm pieces, and their geometrical area was delimited using dielectric tape.

Biosensor functionalization assays

To prepare the electrochemical biosensor, the nectin-1 receptor was first immobilized onto the WE through the drop-casting method. Briefly, 4.0 μL of 1.0 mg mL^{-1} PEI solution prepared in deionized water was gently deposited on the WE and dried for 60 min at 37°C. Next, 4.6 μL of 0.13 mg mL^{-1} nectin-1 receptor containing 25.0 mmol L^{-1} EDC and 50.0 mmol L^{-1} of NHS solution prepared in 0.1 mol L^{-1} PBS (pH = 7.4) was deposited on the surface of the PEI-modified WE and incubated at 37°C for 30 min. Subsequently, the remaining unmodified zones of the WE were blocked with 4.0 μL of 1.0% (m/v) BSA solution prepared in deionized water, and the devices were stored for 30 min at 37°C to dry. This step aims to prevent nonspecific interactions of the sample with the biosensor's surface. Finally, 4.0 μL of chitosan 0.5% (m/v), prepared in 2% (v/v) acetic acid, was deposited onto the WE. The biosensor was incubated at 37°C for 60 min and then washed with 0.1 mol L^{-1} PBS (pH = 7.4) before use.

Collection of vaginal swab samples from HSV-2-infected guinea pigs

In guinea pigs, vaginal infection with HSV-2 causes a clinical disease similar to that in humans; this model is described in detail elsewhere.⁵⁶ Briefly, female guinea pigs were infected intravaginally with HSV-2 MS strain (5×10^5 PFU) in a 50 μL inoculum volume. Mock infections were used as controls. Vaginal swabs, collected on day 2, were stored at -80°C in 1 mL DMEM containing heat-inactivated 5% FBS and an antibiotics/antimycotics cocktail.⁵⁶ The samples were quantified for the replicating virus by incubating serial 10-fold dilutions of each of the swab samples onto Vero cells for 1 h in an incubator under 5% CO_2 at 37°C. Dilutions of the samples were removed after 1 h and overlaid with 1.5% methylcellulose in DMEM supplemented with 5% FBS and incubated for 72 h in the same incubator. The overlay was removed, and 0.1% crystal violet in 25% methanol was added to the cells. Plaques were counted under the microscope and calculated as PFU mL^{-1} .⁵⁷

HSV-2 biosensing

For the HSV-2 biosensing, 10.0 μL of 0.1 mol L^{-1} PBS (pH = 7.4) or DMEM containing either gD2 or HSV-2 samples was applied to the electrochemical cell to cover the surface of the WE. The electrochemical cells were incubated at room temperature for 5 min, and then the electrochemical cell was washed with PBS (0.1 mol L^{-1} ; pH = 7.4) to remove unbound components. Then, the redox probe (200 μL of a 5.0 mmol L^{-1} $[\text{Fe}(\text{CN})_6]^{3-/4-}$ in 0.1 mol L^{-1} KCl solution) was used for the EIS measurements. The R_{CT} values were calculated with the use of the Randles equivalent electrical circuit on the Nyquist plots. The HSV-2 samples were heat-inactivated (56°C for 1 h) prior to the analysis.

Reproducibility, stability, and cross-reactivity studies

Reproducibility was studied with six biosensors, each having electrodes manufactured from different batches. Biosensors were exposed to 1.0 ng mL^{-1} of gD2 and incubated for 5 min. The analytical signals (R_{CT} values) obtained for these six devices were used to calculate the RSD. The stability of the biosensors stored at 25°C, -20°C , or 4°C was evaluated over 7 days by extracting the analytical sensitivity parameter from analytical curves at concentrations of gD2 ranging from 1×10^{-12} to 1×10^{-10} g mL^{-1} . The cross-reactivity

studies used the same optimized condition as used for HSV-2 detection, with five viruses, all at 10^5 PFU mL⁻¹ except for MHV, which was at 10^8 PFU mL⁻¹: H1N1 (A/California/2009), influenza B (B/Colorado), H3N2, MHV-mouse hepatitis virus, and SARS-CoV-2 prepared in viral transport medium (VTM).

Supplementary Material

Refer to Web version on PubMed Central for supplementary material.

ACKNOWLEDGMENTS

C.F.N. holds a Presidential Professorship at the University of Pennsylvania, is a recipient of the Langer Prize by the AIChE Foundation, and acknowledges funding from the Procter & Gamble Company, United Therapeutics, a BBRF Young Investigator Grant, and the Defense Threat Reduction Agency (DTRA; HDTRA11810041 and HDTRA1-21-1-0014). Research reported in this publication was supported by the Nemirovsky Prize, the National Institute of General Medical Sciences of the National Institutes of Health under award number R35GM138201, Penn Health-Tech Accelerator Award, the IADR Innovation in Oral Care Award, and by funds provided by the Dean's Innovation Fund from the Perelman School of Medicine at the University of Pennsylvania (all to C.F.N.). H.M.F. acknowledges the NIAID RO1 grant 139618. W.R.d.A. acknowledges funding from Brazilian funding agencies CAPES (88887.479793/2020-00), FAPESP (2022/03250-7, and 2018/08782-1), FAEPEX/PRP/UNICAMP (3374/19), and CNPq (438828/2018-6) for supporting the research. Figures 1 and 3 and graphical abstract were prepared in BioRender.com. We thank Dr. Susan Weiss' Lab for kindly donating the following strains: H1N1 (A/California/2009), influenza B (B/Colorado), H3N2, and MHV-mouse hepatitis virus. We also thank Dr. Ronald Collman for kindly donating SARS-CoV-2 samples. We thank the de la Fuente Lab for insightful discussions, Dr. Karen Pepper for editing the manuscript, and Dr. Jon Epstein for his support.

REFERENCES

1. James C, Harfouche M, Welton NJ, Turner KM, Abu-raddad LJ, Gottlieb SL, and Looker KJ (2020). Herpes simplex virus: global infection prevalence and incidence estimates. *Bull. World Health Organ* 98, 315–329. 10.1086/342104. [PubMed: 32514197]
2. Weidmann M, Meyer-König U, and Hufert FT (2003). Rapid detection of herpes simplex virus and varicella-zoster virus infections by real-time PCR. *J. Clin. Microbiol* 41, 1565–1568. 10.1128/JCM.41.4.1565-1568.2003. [PubMed: 12682146]
3. Herold BC, Visalli RJ, Susmarski N, Brandt CR, and Spear PG (1994). Glycoprotein C-independent binding of herpes simplex virus to cells requires cell surface heparan sulphate and glycoprotein B. *J. Gen. Virol* 75, 1211–1222. 10.1099/0022-1317-75-6-1211. [PubMed: 8207388]
4. WuDunn D, and Spear PG (1989). Initial interaction of herpes simplex virus with cells is binding to heparan sulfate. *J. Virol* 63, 52–58. 10.1128/jvi.63.1.52-58.1989. [PubMed: 2535752]
5. Nicola AV, Peng C, Lou H, Cohen GH, and Eisenberg RJ (1997). Antigenic structure of soluble herpes simplex virus (HSV) glycoprotein D correlates with inhibition of HSV infection. *J. Virol* 71, 2940–2946. 10.1128/jvi.71.4.2940-2946.1997. [PubMed: 9060653]
6. Eisenberg RJ, Atanasiu D, Cairns TM, Gallagher JR, Krummenacher C, and Cohen GH (2012). Herpes virus fusion and entry: A story with many characters. *Viruses* 4, 800–832. 10.3390/v4050800. [PubMed: 22754650]
7. Johnson RM, and Spear PG (1989). Herpes simplex virus glycoprotein D mediates interference with herpes simplex virus infection. *J. Virol* 63, 819–827. 10.1128/jvi.63.2.819-827.1989. [PubMed: 2536105]
8. Johnson DC, Burke RL, and Gregory T (1990). Soluble forms of herpes simplex virus glycoprotein D bind to a limited number of cell surface receptors and inhibit virus entry into cells. *J. Virol* 64, 2569–2576. 10.1128/jvi.64.6.2569-2576.1990. [PubMed: 2159532]
9. Fuller AO, and Lee WC (1992). Herpes simplex virus type 1 entry through a cascade of virus-cell interactions requires different roles of gD and gH in penetration. *J. Virol* 66, 5002–5012. 10.1128/jvi.66.8.5002-5012.1992. [PubMed: 1321283]

10. Singh A, Preiksaitis J, Ferenczy A, and Romanowski B (2005). The laboratory diagnosis of herpes simplex virus infections. *Can. J. Infect Dis. Med. Microbiol* 16, 92–98. 10.1155/2005/318294. [PubMed: 18159535]
11. Anderson NW, Buchan BW, and Ledebor NA (2014). Light Microscopy, Culture, Molecular, and Serologic Methods for Detection of Herpes Simplex Virus. *J. Clin. Microbiol* 52, 2–8. 10.1128/JCM.01966-13. [PubMed: 24131689]
12. Wald A, and Ashley-Morrow R (2002). Serological testing for herpes simplex virus (HSV)-1 and HSV-2 infection. *Clin. Infect. Dis* 35, S173–S182. 10.1086/342104. [PubMed: 12353203]
13. Johnson G, Nelson S, Petric M, and Tellier R (2000). Comprehensive PCR-based assay for detection and species identification of human herpesviruses. *J. Clin. Microbiol* 38, 3274–3279. 10.1128/jcm.38.9.3274-3279.2000. [PubMed: 10970370]
14. Gardella C, Huang ML, Wald A, Magaret A, Selke S, Morrow R, and Corey L (2010). Rapid polymerase chain reaction assay to detect herpes simplex virus in the genital tract of women in labor. *Obstet. Gynecol* 115, 1209–1216. 10.1097/AOG.0b013e3181e01415. [PubMed: 20502292]
15. Narang J, Singhal C, Mathur A, Sharma S, Singla V, and Pundir CS (2018). Portable bioactive paper based genosensor incorporated with Zn-Ag nanoblocks for herpes detection at the point-of-care. *Int. J. Biol. Macromol* 107, 2559–2565. 10.1016/j.ijbiomac.2017.10.146. [PubMed: 29107138]
16. Tam PD, Tuan MA, Aarnink T, and Chien ND (2008). Directly immobilized DNA sensor for label-free detection of herpes virus In 2008 International Conference on Technology and Applications in Biomedicine (ITAB), pp. 214–218. 10.1109/ITAB.2008.4570538.
17. Kara P, Meric B, Zeytinoglu A, and Ozsoz M (2004). Electrochemical DNA biosensor for the detection and discrimination of herpes simplex Type I and Type II viruses from PCR amplified real samples. *Anal. Chim. Acta X* 518, 69–76. 10.1016/j.aca.2004.04.004.
18. Klunder KJ, Nilsson Z, Sambur JB, and Henry CS (2017). Patternable Solvent-Processed Thermoplastic Graphite Electrodes. *J. Am. Chem. Soc* 139, 12623–12631. 10.1021/jacs.7b06173. [PubMed: 28797166]
19. Giovine P, Settembre EC, Bhargava AK, Luftig MA, Lou H, Cohen GH, Eisenberg RJ, Krummenacher C, and Carfi A (2011). Structure of herpes simplex virus glycoprotein d bound to the human receptor nectin-1. *PLoS Pathog* 7, 1–12. 10.1371/journal.ppat.1002277.
20. Torres MDT, de Araujo WR, de Lima LF, Ferreira AL, and de la Fuente-Nunez C (2021). Low-cost biosensor for rapid detection of SARS-CoV-2 at the point of care. *Matter* 4, 2403–2416. 10.1016/j.matt.2021.05.003. [PubMed: 33997767]
21. Randles JEB (1947). Kinetics of rapid electrode reactions. *Faraday Discuss* 1, 11–19. 10.1039/DF9470100011.
22. de Lima LF, Ferreira AL, Torres MDT, de Araujo WR, and de la Fuente-Nunez C (2021). Minute-scale detection of SARS-CoV-2 using a low-cost biosensor composed of pencil graphite electrodes. *Proc. Natl. Acad. Sci. USA* 118. e2106724118–e2106724119. 10.1073/pnas.2106724118. [PubMed: 34244421]
23. Ferreira AL, de Lima LF, Moraes AS, Rubira RJ, Constantino CJ, Leite FL, Delgado-Silva AO, and Ferreira M (2021). Development of a novel biosensor for Creatine Kinase (CK-MB) using Surface Plasmon Resonance (SPR). *Appl. Surf. Sci* 554, 149565. 10.1016/j.apsusc.2021.149565.
24. Balint R, Cassidy NJ, and Cartmell SH (2014). Conductive polymers: Towards a smart biomaterial for tissue engineering. *Acta Biomater* 10, 2341–2353. 10.1016/j.actbio.2014.02.015. [PubMed: 24556448]
25. Li J, Bai J, Dong L, Yang M, Hu Y, Gao L, and Qian H (2021). A Novel Electrochemical Biosensor based on Layered Hydroxide Nanosheets/DNA Composite for the Determination of Phenformin Hydrochloride. *Int. J. Electrochem. Sci* 16, 210237. 10.20964/2021.02.05.
26. Farooq U, Ullah MW, Yang Q, Aziz A, Xu J, Zhou L, and Wang S (2020). High-density phage particles immobilization in surface-modified bacterial cellulose for ultra-sensitive and selective electrochemical detection of *Staphylococcus aureus*. *Biosens. Bioelectron* 157, 112163. 10.1016/j.bios.2020.112163. [PubMed: 32250935]
27. Deng C, Chen J, Nie Z, and Si S (2010). A sensitive and stable biosensor based on the direct electrochemistry of glucose oxidase assembled layer-by-layer at the multiwall carbon nanotube-

- modified electrode. *Biosens. Bioelectron* 26, 213–219. 10.1016/j.bios.2010.06.013. [PubMed: 20620040]
28. Cruz J, Kawasaki M, and Gorski W (2000). Electrode coatings based on chitosan scaffolds. *Anal. Chem* 72, 680–686. 10.1021/ac990954b. [PubMed: 10701250]
29. Hanssen BL, Siraj S, and Wong DK (2016). Recent strategies to minimise fouling in electrochemical detection systems. *Rev. Anal. Chem* 35, 1–28. 10.1515/revac-2015-0008.
30. Annu, and Raja AN (2020). Recent development in chitosan-based electrochemical sensors and its sensing application. *Int. J. Biol. Macromol* 164, 4231–4244. 10.1016/j.ijbiomac.2020.09.012. [PubMed: 32918960]
31. Suginta W, Khunkaewla P, and Schulte A (2013). Electrochemical Biosensor Applications of Polysaccharides Chitin and Chitosan. *Chem. Rev* 113, 5458–5479. 10.1021/cr300325r. [PubMed: 23557137]
32. Hlavatá L, Vyskočil V, Beníková K, Borbélyová M, and Labuda J (2014). DNA-based biosensors with external Nafion and chitosan membranes for the evaluation of the antioxidant activity of beer, coffee, and tea. *Open Chem* 12, 604–611. 10.2478/s11532-014-0516-4.
33. Yang L, Ren X, Tang F, and Zhang L (2009). A practical glucose biosensor based on Fe₃O₄ nanoparticles and chitosan/nafion composite film. *Biosens. Bioelectron* 25, 889–895. 10.1016/j.bios.2009.09.002. [PubMed: 19781932]
34. Kang H, Jung S, Jeong S, Kim G, and Lee K (2015). Polymer-metal hybrid transparent electrodes for flexible electronics. *Nat. Commun* 6, 6503–6507. 10.1038/ncomms7503. [PubMed: 25790133]
35. Farmani MR, Peyman H, and Roshanfekr H (2020). Blue luminescent graphene quantum dot conjugated cysteamine functionalized-gold nanoparticles (GQD-AuNPs) for sensing hazardous dye. *Spectrochim. Acta Mol. Biomol. Spectrosc* 229, 117960. 10.1016/j.saa.2019.117960.
36. Gottschalk PG, and Dunn JR (2005). The five-parameter logistic: A characterization and comparison with the four-parameter logistic. *Anal. Biochem* 343, 54–65. 10.1016/j.ab.2005.04.035. [PubMed: 15953581]
37. Holstein CA, Griffin M, Hong J, and Sampson PD (2015). Statistical Method for Determining and Comparing Limits of Detection of Bioassays. *Anal. Chem* 87, 9795–9801. 10.1021/acs.analchem.5b02082. [PubMed: 26376354]
38. Tam PD, Tuan MA, Huy TQ, Le AT, and Hieu NV (2010). Facile preparation of a DNA sensor for rapid herpes virus detection. *Mater. Sci. Eng. C* 30, 1145–1150. 10.1016/j.msec.2010.06.010.
39. Toldrà A, Furones MD, O'Sullivan CK, and Campàs M (2020). Detection of isothermally amplified ostreid herpesvirus 1 DNA in Pacific oyster (*Crassostrea gigas*) using a miniaturised electrochemical biosensor. *Talanta* 207, 120308. 10.1016/j.talanta.2019.120308. [PubMed: 31594570]
40. Garcia LF, Silvio Batista Rodrigues E, Rocha Lino de Souza G, Jubé Wastowski I, Mota de Oliveira F, Torres Pio dos Santos W, and Souza Gil E (2020). Impedimetric Biosensor for Bovine Herpesvirus Type 1-Antigen Detection. *Electroanalysis* 32, 1100–1106. 10.1002/elan.201900606.
41. Loughman T, Singh B, Seddon B, Noone P, and Santhosh P (2017). Validation of a membrane touch biosensor for the qualitative detection of IgG class antibodies to herpes simplex virus type 2. *Analyst* 142, 2725–2734. 10.1039/C7AN00666G. [PubMed: 28708188]
42. Nahar S, Ahmed MU, Safavieh M, Rochette A, Toro C, and Zourob M (2015). A flexible and low-cost polypropylene pouch for naked-eye detection of herpes simplex viruses. *Analyst* 140, 931–937. 10.1039/c4an01701c. [PubMed: 25529059]
43. Kessler HH, Mühlbauer G, Rinner B, Stelzl E, Berger A, Dörr HW, Santner B, Marth E, and Rabenau H (2000). Detection of herpes simplex virus DNA by real-time PCR. *J. Clin. Microbiol* 38, 2638–2642. 10.1128/jcm.38.7.2638-2642.2000. [PubMed: 10878056]
44. Perkins JD (2007). Detection and Diagnosis of Herpes Simplex Virus Infection in Adults with Acute Liver Failure. *Liver Transplant* 13, 767–768.
45. Burrows J, Nitsche A, Bayly B, Walker E, Higgins G, and Kok T (2002). Detection and subtyping of Herpes simplex virus in clinical samples by LightCycler PCR, enzyme immunoassay and cell culture. *BMC Microbiol* 2, 12–17. 10.1186/1471-2180-2-12. [PubMed: 12069697]

46. Dominguez SR, Pretty K, Hengartner R, and Robinson CC (2018). Comparison of herpes simplex virus PCR with culture for virus detection in multisource surface swab specimens from neonates. *J. Clin. Microbiol* 56, e00632-18–e00635. 10.1128/JCM.00632-18. [PubMed: 29875197]
47. Krumbholz A, Schäfer M, Lorentz T, and Sauerbrei A (2019). Quadruplex real-time PCR for rapid detection of human alphaherpesviruses. *Med. Microbiol. Immunol* 208, 197–204. 10.1007/s00430-019-00580-2. [PubMed: 30680459]
48. MultiCode[®]-RTx Herpes Simplex Virus 1 & 2 Kit, Real-Time PCR Qualitative Detection and Typing of HSV-1 or HSV-2, Luminex Corporation.
49. BD ProbeTec[™] Herpes Simplex Viruses (HSV 1 & 2) Qx Amplified DNA Assays, BD Diagnostic Systems, Becton Dickinson & CO.
50. Kim HJ, Tong Y, Tang W, Quimson L, Cope VA, Pan X, Motre A, Kong R, Hong J, Kohn D, et al. (2011). A rapid and simple isothermal nucleic acid amplification test for detection of herpes simplex virus types 1 and 2. *J. Clin. Virol* 50, 26–30. 10.1016/J.JCV.2010.09.006. [PubMed: 20947417]
51. Geraghty RJ, Fridberg A, Krummenacher C, Cohen GH, Eisenberg RJ, and Spear PG (2001). Use of chimeric nectin-1(HveC)-related receptors to demonstrate that ability to bind alphaherpesvirus gD is not necessarily sufficient for viral entry. *Virology* 285, 366–375. 10.1006/viro.2001.0989. [PubMed: 11437670]
52. Ferreira AL, de Lima LF, Torres MDT, de Araujo WR, and de la Fuente-Nunez C (2021). Low-Cost Optodiagnostic for Minute-Time Scale Detection of SARS-CoV-2. *ACS Nano* 15, 17453–17462. 10.1021/acsnano.1c03236. [PubMed: 34669371]
53. Elveborg S, Monteil VM, and Mirazimi A (2022). Methods of Inactivation of Highly Pathogenic Viruses for Molecular, Serology or Vaccine Development Purposes. *Pathogens* 11, 271. 10.3390/pathogens11020271. [PubMed: 35215213]
54. Carfí A, Willis SH, Whitbeck JC, Krummenacher C, Cohen GH, Eisenberg RJ, and Wiley DC (2001). Herpes Simplex Virus Glycoprotein D Bound to the Human Receptor. *Mol. Cell* 8, 169–179. 10.1016/S1097-2765(01)00298-2. [PubMed: 11511370]
55. Krummenacher C, Nicola AV, Whitbeck JC, Lou H, Hou W, Lambris JD, Geraghty RJ, Spear PG, Cohen GH, and Eisenberg RJ (1998). Herpes Simplex Virus Glycoprotein D Can Bind to Poliovirus Receptor-Related Protein 1 or Herpesvirus Entry Mediator, Two Structurally Unrelated Mediators of Virus Entry. *J. Virol* 72, 7064–7074. 10.1128/JVI.72.9.7064-7074.1998. [PubMed: 9696799]
56. Hook LM, Harvey M, and Friedman SA (2021). Guinea Pig and Mouse Models for Genital Herpes Infection. *Curr Protoc* 1, 32.
57. Awasthi S, Hook LM, Shaw CE, Pahar B, Stagray JA, Liu D, Veazey RS, and Friedman HM (2017). An HSV-2 Trivalent Vaccine Is Immunogenic in Rhesus Macaques and Highly Efficacious in Guinea Pigs. *PLoS Pathog* 13, e1006141. 10.1371/journal.ppat.1006141. [PubMed: 28103319]

Highlights

Ultrasensitive electrochemical biosensor for herpes simplex virus (HSV) detection

The biosensor enables rapid and accurate detection of HSV within minutes

The biosensor is inexpensive (\$1 USD per test) compared to existing HSV detection methods

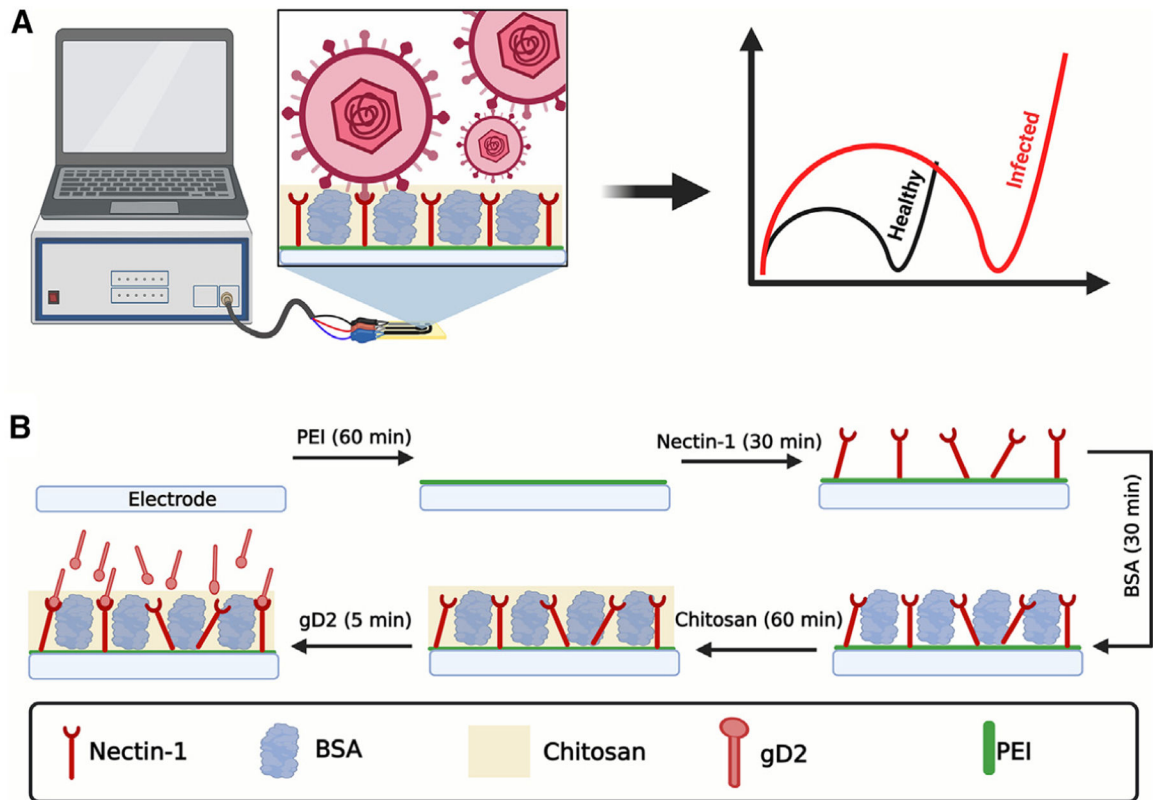


Figure 1. Detection and functionalization approach of the herpes virus electrochemical biosensor
 (A) Schematic representation of the HSV sensing using the electrochemical biosensor.
 (B) Functionalization and optimization steps of the electrochemical biosensor. This figure was created in [BioRender.com](https://www.biorender.com).

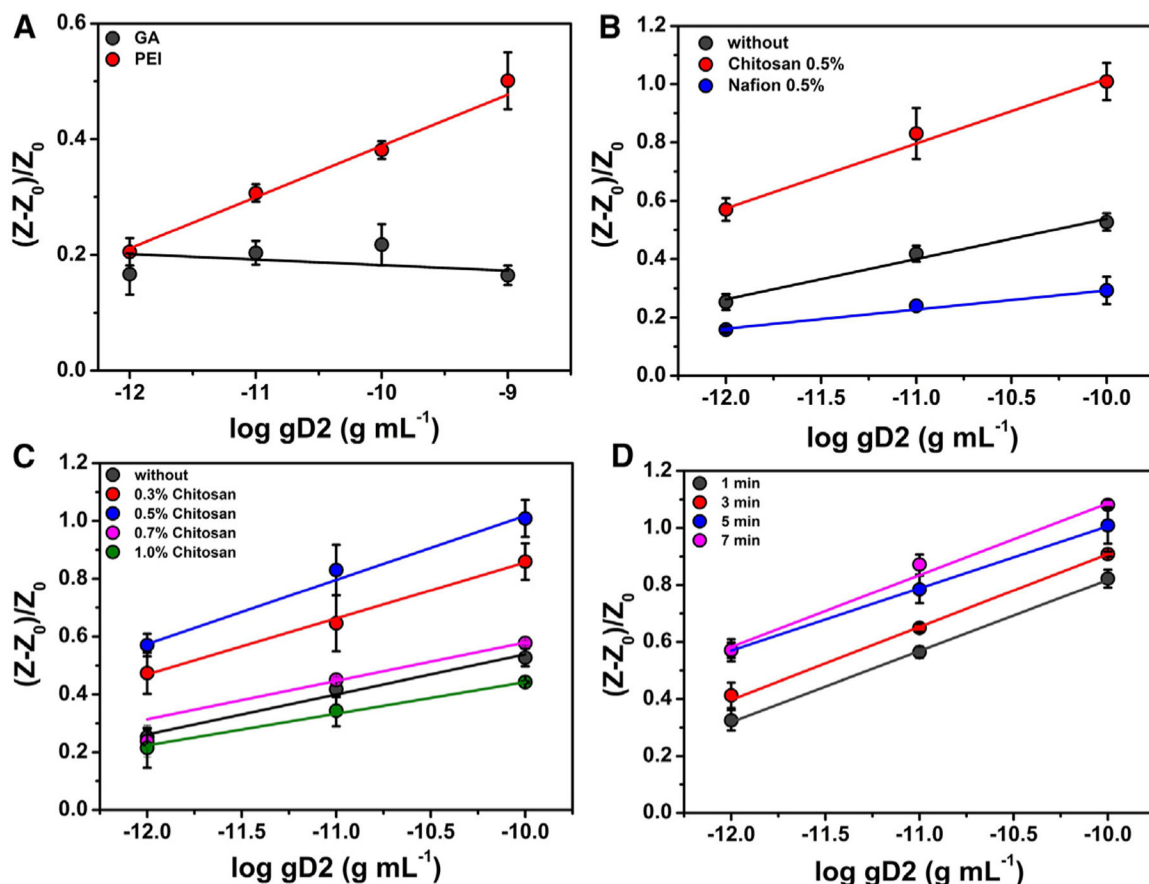


Figure 2. Optimization studies of the herpes virus electrochemical biosensor

(A) Anchoring of nectin-1 using 25% (m/v) GA (black circles) and 1.0 mg mL⁻¹ PEI (red circles). Optimal results were obtained when the substrate was modified with PEI to enable the anchoring of the nectin-1 receptor through the -COOH terminal group.

(B) Analytical response of the biosensor when fabricated without an additional membrane layer (black circles), modified with 0.5% (m/v) chitosan (red circles), and modified with 0.5% (m/v) Nafion (blue circles). The highest sensitivity was obtained when the biosensor was modified with 0.5% (m/v) chitosan.

(C) Effect of chitosan concentration on biosensor sensitivity: 0.0% (black circles), 0.3% (m/v; red circles), 0.5% (m/v; blue circles), 0.7% (m/v; pink circles), and 1.0% (m/v; green circles). Chitosan at 0.5% (m/v) provided the highest detectability maintaining the lowest reagent-to-usage ratio; thus, this condition was selected for subsequent measurements.

(D) Incubation time experiments between gD2 and the modified electrochemical biosensor. Calibration curves were generated using gD2 at concentrations ranging from 1 pg mL⁻¹ to 0.1 ng mL⁻¹ and incubation times ranging from 1 to 7 min. No significantly increased differences in the detectability of gD2 were observed for incubation periods longer than 5 min; thus, this incubation time was selected for subsequent work. All experiments were carried out at room temperature in triplicate (n = 3) and obtained through calibration curves for gD2 at a concentration range between 1.0 pg mL⁻¹ and 0.1 ng mL⁻¹. The error bars correspond to the standard deviation. All EIS measurements were recorded at open circuit

potential at the frequency range of 1.3×10^5 Hz to 0.1 Hz and using an amplitude of 10 mV in the following medium: $5 \text{ mmol L}^{-1} [\text{Fe}(\text{CN})_6]^{3-/4-}$ in 0.1 mol L^{-1} KCl solution.

Author Manuscript

Author Manuscript

Author Manuscript

Author Manuscript

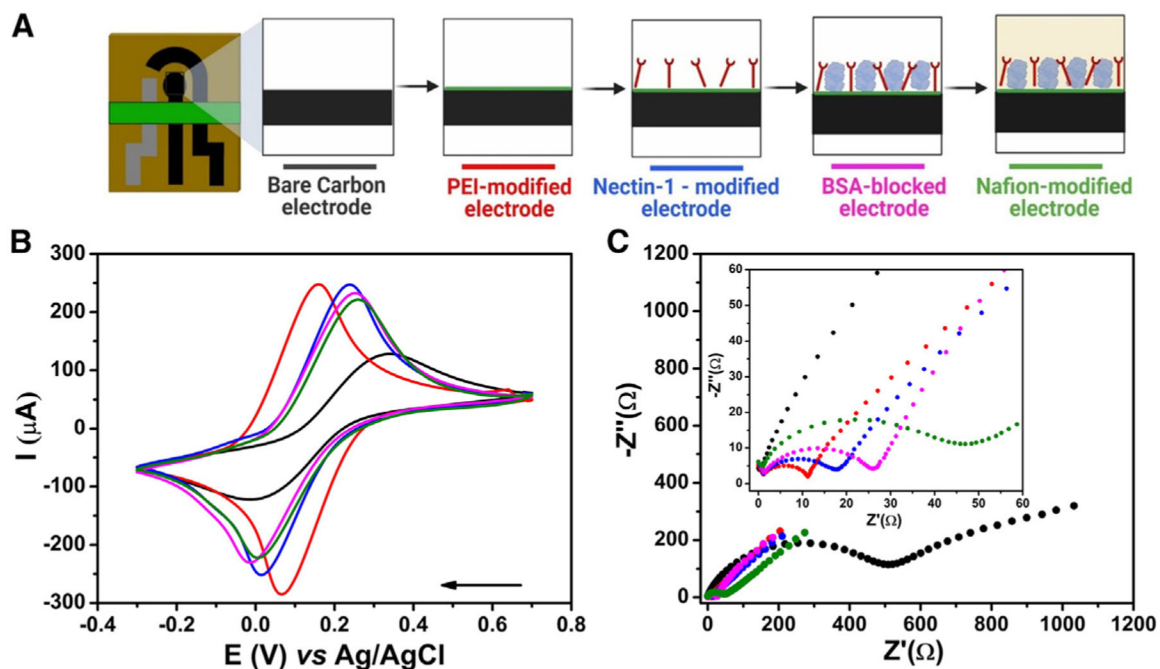


Figure 3. Functionalization steps and electrochemical characterization of the biosensor
 (A) Schematic representation of the stepwise functionalization of the electrochemical biosensor.

(B) CV experiments were recorded for each modification step made to the biosensor surface in a solution of $5.0 \text{ mmol L}^{-1} [\text{Fe}(\text{CN})_6]^{3-/4-}$ containing $0.1 \text{ mol L}^{-1} \text{ KCl}$ as the supporting electrolyte. A potential window from -0.3 V to 0.7 V and a scan rate of 50 mV s^{-1} were used.

(C) Nyquist plots were obtained using the same conditions as those shown in (A). Inset shows a zoomed-in view of the plots at high-frequency regions. Conditions used were frequency range from $1 \times 10^5 \text{ Hz}$ to 0.1 Hz and 10 mV amplitude. Measurements were performed at room temperature. The colors displayed in the CV and Nyquist plots correspond to each modification step outlined in (A). This figure was partially created in BioRender.com.

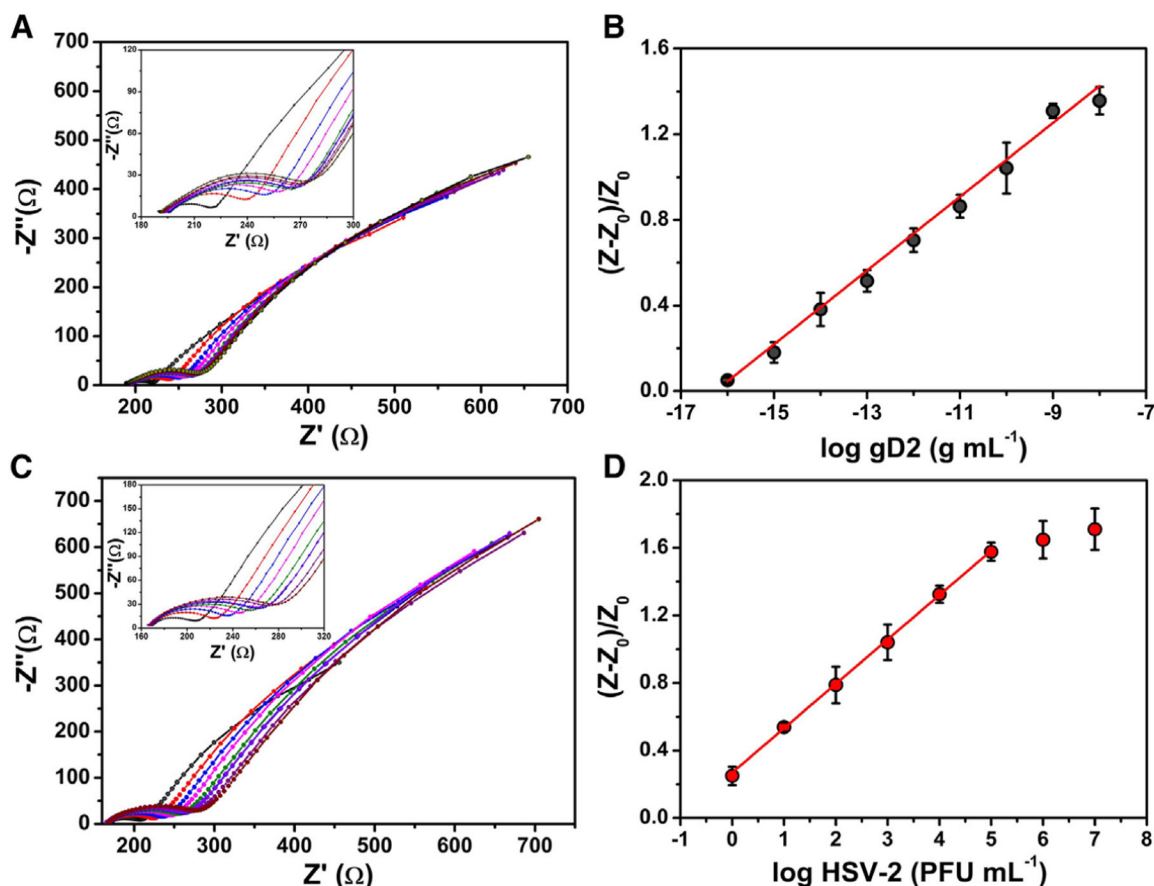


Figure 4. Analytical curves for HSV-2 detection

(A) Nyquist plots for gD2 at concentrations ranging from 0.1 fg mL⁻¹ to 10.0 ng mL⁻¹ in 0.1 mol L⁻¹ PBS (pH = 7.4).

(B) Dose-response curve obtained from normalized R_{CT} values extracted from Nyquist plots as a function of the logarithm of the gD2 concentration.

(C) Nyquist plots for titered HSV-2 viral solution at levels ranging from 1×10^0 PFU mL⁻¹ to 1×10^7 PFU mL⁻¹.

(D) Dose-response curve obtained from normalized R_{CT} values extracted from Nyquist plots as a function of the logarithm of the HSV-2 viral loads. The EIS measurements were performed in triplicate in 5.0 mmol L⁻¹ [Fe(CN)₆]^{3-/4-} and a 0.1 mol L⁻¹ KCl solution applying the open circuit potential at a frequency range of 1×10^5 Hz to 0.1 Hz and using an amplitude of 10 mV. All measurements were recorded in triplicate ($n = 3$), using 10 μ L of gD2 or HSV-2 samples (from 1×10^0 PFU mL⁻¹ to 1×10^7 PFU mL⁻¹), and samples were incubated for 5 min on the biosensor surface. The error bars correspond to the standard deviation.

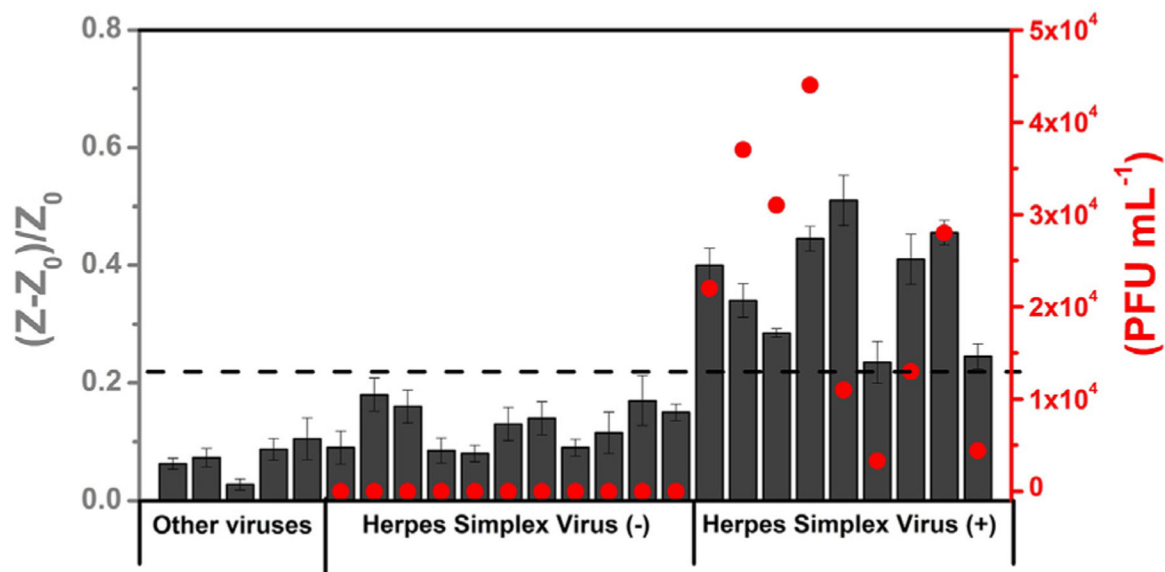


Figure 5. Detection of HSV-2 in biofluid samples from guinea pigs

Comparison of the electrochemical biosensor response (normalized R_{CT} values) obtained for the cross-reactivity studies (other viruses) in VTM and the analyses of 20 guinea pig vagina samples in DMEM (11 HSV-2 negative and 9 HSV-2 positive) (dark gray bars) and quantification of the HSV-2-positive samples obtained using the conventional titrated method (red circles) and shown as PFU mL^{-1} . The dotted line indicates the cutoff value of the normalized R_{CT} response established to indicate whether the sample was identified as positive for HSV-2 by our biosensor. All electrochemical measurements were recorded in triplicate ($n = 3$), and the error bars correspond to the standard deviation.

Table 1.

Comparison of the analytical parameters in various methods reported for the detection of herpes viruses

Method	LOD	Technique	Target	Working concentration range	Time (min)	Reference
Our method	0.057 PFU mL ⁻¹	EIS	HSV-2	1 × 10 ⁰ to 1 × 10 ⁷ PFU mL ⁻¹	9	This work
	0.019 fg mL ⁻¹	EIS	gD2	0.1 fg mL ⁻¹ to 10.0 ng mL ⁻¹		
PEGE and MDB/DNA	14.77 fmol mL ⁻¹	DPV	DNA	1 to 20 µg mL ⁻¹	35 ^a	Kara et al. ¹⁷
Ppy/DNA film	50.0 fmol mL ⁻¹	Conductivity	DNA	2.0 to 24.0 pmol mL ⁻¹	–	Tam et al. ³⁸
RPA/Au/DNA	207 copies	Amperometry	DNA	1 × 10 ¹ to 1 × 10 ⁸ copies	35	Toldrà et al. ³⁹
Impedimetric immunosensor	0.66 TCID ₅₀ mL ⁻¹	EIS	BHV-1	10.0–50.0 TCID ₅₀ mL ⁻¹	10 ^b	Garcia et al. ⁴⁰
Biochip	–	Coulometric	IgG	–	65	Loughman et al. ⁴¹
Smart cup	100 copies mL ⁻¹	LAMP	DNA	1 × 10 ⁰ to 1 × 10 ³ PFU mL ⁻¹	30	Nahar et al. ⁴²
PP/DNA	0.61 copies mL ⁻¹	LAMP	DNA	10 ⁴ PFU mL ⁻¹ to 100 PFU mL ⁻¹	45	Narang et al. ¹⁵
EPAD/Zn-Ag nanoblooms/DNA	97.0 copies mL ⁻¹	CV	DNA	113–10 ³ and 3 × 10 ⁵ –1×10 ⁶ copies mL ⁻¹	120 ^c	Kessler et al. ⁴³
LC/DNA	1 × 10 ⁴ copies mL ⁻¹	PCR	DNA	2 × 10 ³ to 5 × 10 ³ copies mL ⁻¹	30	Weidmann et al. ²
LC/DNA	10.0 copies mL ⁻¹	PCR	DNA	–	150	Perkins et al. ⁴⁴
LC/DNA	between 1 and 5 copies/reaction	PCR	DNA	3.5 to 36 × 10 ⁸ copies mL ⁻¹	–	Burrows et al. ⁴⁵
LC/DNA	4 copies µL ⁻¹	PCR	DNA	–	<60	Dominguez et al. ⁴⁶
LC/DNA	1 copy mL ⁻¹	PCR	DNA	18.0 to 35.9 Ct	–	Tam et al. ³⁸
LC/DNA	1.2 to 5.8 copies/test	RT-PCR	DNA	–	90	Krumbholz et al. ⁴⁷
MultiCode -RTx HSV 1&2 Kit	–	RT-PCR	DNA	–	240	MultiCode-RTx Herpes Simplex Virus 1 & 2 Kit, Real-Time PCR Qualitative Detection and Typing of HSV-1 or HSV-2 ⁴⁸
BD ProbeTec HSV Qx test	–	RT-PCR	DNA	–	160	BD ProbeTec Herpes Simplex Viruses (HSV 1 & 2) Qx Amplified DNA Assays ⁴⁹
IsoAmp HSV assay	34.1 copies/test	HDA-LFA	DNA	–	90	Kim et al. ⁵⁰

PEGE, pencil graphite electrodes; MDB, Meldola blue; DPV, differential pulse voltammetry; LAMP, loop-mediated isothermal amplification; PP, polypropylene; EPAD, electrochemical paper-based analytical device; CV, cyclic voltammetry; LC, LightCycler; PCR, polymerase chain reaction; GE, genome equivalents; OsHV-1, ostreid herpesvirus 1; RPA, isothermal recombinase polymerase amplification; Au, gold electrode; BHV-1, bovine herpesvirus type 1; HDA-LFA, helicase-dependent amplification and lateral-flow analysis.

^aTesting time considering only hybridization and accumulation processes.

^bConsidering only the sample incubation.

^cConsidering only the hybridization step.